

Robust Multivariate Functional Control Charts

Christian Capezza¹, Fabio Centofanti ^{*1}, Antonio Lepore¹, and Biagio Palumbo¹

¹*Department of Industrial Engineering, University of Naples Federico II, Piazzale Tecchio 80, 80125, Naples, Italy*

Abstract

Profile monitoring assesses the stability over time of one or multiple functional quality characteristics to quickly detect special causes of variation that act on a process. In modern Industry 4.0 applications, a huge amount of data is acquired during manufacturing processes that are often contaminated with anomalous observations in the form of both casewise and cellwise outliers. Because anomalous observations can seriously affect the monitoring performance, profile monitoring methods that are able to successfully deal with outliers are needed. To this aim, we propose a new framework, referred to as robust multivariate functional control charts (RoMFCC), that is able to monitor multivariate functional data while being robust to both functional casewise and cellwise outliers. The RoMFCC relies on four main elements: (I) a univariate filter to identify functional cellwise outliers to be replaced by missing components; (II) a robust functional data imputation method of missing values; (III) a casewise robust dimensionality reduction; (IV) a monitoring strategy for the multivariate functional quality characteristic. An extensive Monte Carlo simulation study is performed to quantify the monitoring performance of the RoMFCC by comparing it with some competing methods already available in the literature. Finally, a motivating real-case study is presented where the proposed framework is used to monitor a resistance spot welding process in the automotive industry.

Keywords: Functional Data Analysis, Profile Monitoring, Statistical Process Control, Robust Estimation, Casewise and Cellwise Outliers

*Corresponding author. e-mail: fabio.centofanti@unina.it

1 Introduction

In modern industrial applications, data acquisition systems allow to collect massive amounts of data with high frequency. Several examples may be found in the current Industry 4.0 framework, which is reshaping the variety of signals and measurements that can be gathered during manufacturing processes. The focus in many of these applications is statistical process monitoring (SPM), whose main aim is to quickly detect unusual conditions in a process when special causes of variation act on it, i.e., the process is out-of-control (OC). On the contrary, when only common causes are present, the process is said to be in-control (IC).

In this context, the experimental measurements of the quality characteristic of interest are often characterized by complex and high dimensional formats that can be well represented as functional data or profiles (Ramsay and Silverman, 2005; Kokoszka and Reimherr, 2017). The simplest approach for monitoring one or multiple functional variables is based on the extraction of scalar features from each profile, e.g., the mean, followed by the application of classical SPM techniques for multivariate data (Montgomery, 2012). However, feature extraction is known to be problem-specific, arbitrary, and risks compressing useful information. Thus, there is a growing interest in *profile monitoring* (Noorossana et al., 2011), whose aim is to monitor a process when the quality characteristic is best characterized by one or multiple profiles. Some recent examples of profile monitoring applications can be found in Menafoglio et al. (2018); Capezza et al. (2020, 2021a,b); Centofanti et al. (2021b).

The main tools for SPM are control charts that are implemented in two phases. In Phase I, historical process data are used to set control chart limits to be used in Phase II, i.e., the actual monitoring phase, where observations falling outside the control limits are signaled as OC. In classical SPM applications the historical Phase I data are assumed to come from an IC process. However, this assumption is not always valid. As an example, let consider the motivating real-world application, detailed in Section 4, that concerns the SPM of a resistance spot welding (RSW) process in the assembly of automobiles. RSW is the most common technique employed in joining metal sheets during body-in-white assembly of automobiles (Zhou and Cai, 2014), mainly because of its adaptability for mass production

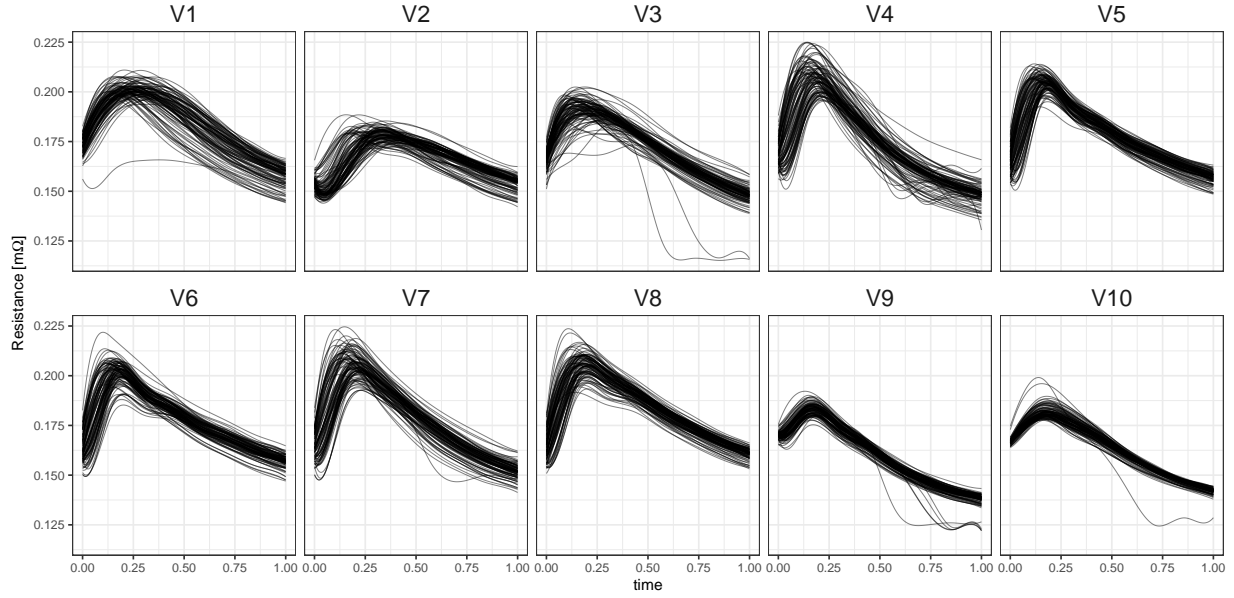


Figure 1: Sample of 100 DRCs, measured in $m\Omega$, that are acquired during the RSW process from the real-case study in Section 4. The different panels refer to the corresponding different spot welds, denoted with names from V1 to V10.

(Martín et al., 2014). Among on-line measurements of RSW process parameters, the so-called dynamic resistance curve (DRC) is recognized as the full technological signature of the metallurgical development of a spot weld (Dickinson et al., 1980; Capezza et al., 2021b) and, thus, can be used to characterize the quality of a finished sub-assembly. Figure 1 shows 100 DRCs corresponding to 10 different spot welds, measured in $m\Omega$, that are acquired during the RSW process from the real-case study presented in Section 4. Several outliers are clearly visible that should be taken into account to set up an effective SPM strategy.

Indeed, control charts are very sensitive to the presence of outlying observations in Phase I that can lead to inflated control limits and reduced power to detect process changes in Phase II. To deal with outliers in the Phase I sample, SPM methods use two common alternatives, namely the diagnostic and the robust approaches (Kruger and Xie, 2012; Hubert et al., 2015). The diagnostic approach is based on standard estimates after the removal of sample units identified as outliers that translates into SPM methods where iterative re-estimation procedures are considered in Phase I. This approach could be often safely applied to eliminate the effect of a small number of very extreme observations. However, it will fail to detect more moderate outliers that are not always as easy to label correctly. On the contrary, the robust approach accepts all the data points and tries to

find a robust estimator which reduces the impact of outliers on the final results (Maronna et al., 2019).

Several robust approaches for the SPM of a multivariate scalar quality characteristic have been proposed in the literature. Alfaro and Ortega (2009) show a comparison of robust alternatives to the classical Hotelling's control chart. It includes two alternative Hotelling's T^2 -type control charts for individual observations, proposed by Vargas (2003) and Jensen et al. (2007), which are based on the minimum volume ellipsoide and the minimum covariance determinant estimators (Rousseeuw, 1984), respectively. Moreover, the comparison includes the control chart based on the reweighted minimum covariance determinant (RMCD) estimators, proposed by Chenouri et al. (2009). More recently, Cabana and Lillo (2021) propose an alternative robust Hotelling's T^2 procedure using the robust shrinkage reweighted estimator.

Although Kordestani et al. (2020) and Moheghi et al. (2020) propose robust estimators to monitoring simple linear profiles, to the best of authors' knowledge, a robust approach able to successfully capture the functional nature of a multivariate functional quality characteristic has not been devised in the SPM literature so far. Beyond the SPM literature, several works have been proposed to deal with outlying functional observations. Several methods extend the classical linear combination type estimators (i.e., L-estimator) (Maronna et al., 2019) to the functional setting to robustly estimate the center of a functional distribution through trimming (Fraiman and Muniz, 2001; Cuesta-Albertos and Fraiman, 2006) and functional data depths (Cuevas and Fraiman, 2009; López-Pintado and Romo, 2011). Sinova et al. (2018) introduce the notion of maximum likelihood type estimators (i.e., M-estimators) in the functional data setting. More recently, Centofanti et al. (2021a) propose a robust functional ANOVA method that reduces the weights of outlying functional data on the results of the analysis.

Regarding functional principal component analysis (FPCA), robust approaches are classified by Boente and Salibián-Barrera (2021) in three groups, depending on the specific property of principal components on which they focus. Methods in the first group perform the eigenanalysis of a robust estimator of the scatter operator, as the spherical principal components method of Locantore et al. (1999) and the indirect approach of Sawant et al.

(2012). The latter performs a robust PCA method, e.g., ROBPCA (Hubert et al., 2005), on the matrix of the basis coefficients corresponding to a basis expansion representation of the functional data. The second group includes projection-pursuit approaches (Hyndman and Ullah, 2007), which sequentially search for the directions that maximize a robust estimator of the spread of the data projections. Whereas, the third group is composed of methods that estimate the principal components spaces by minimizing a robust reconstruction error measure (Lee et al., 2013). Finally, it is worth mentioning diagnostic approaches for functional outlier detection, which have been proposed for both univariate (Hyndman and Shang, 2010; Arribas-Gil and Romo, 2014; Febrero et al., 2008) and multivariate functional data (Hubert et al., 2015; Dai and Genton, 2018; Alemán-Gómez et al., 2022).

In presence of many functional variables, the lack of robust approaches that deal with outliers is exacerbated by the curse of dimensionality. Traditional multivariate robust estimators assume a casewise contamination model for the data, which consists in a mixture of two distributions, where the majority of the cases is free of contamination and the minority mixture component describes an unspecified outlier generating distribution. Alqallaf et al. (2009) show that these traditional estimators are affected by the problem of propagation of outliers. In situations where only a small number of cases are contaminated, the traditional robust approaches work well. However, under an independent contamination model such as cellwise outliers (i.e., contamination in each variable is independent from the other variables), when the dimensionality of the data is high, the fraction of perfectly observed cases can be rather small and the traditional robust estimators may fail. Moreover, Agostinelli et al. (2015) point out that both types of data contamination, casewise and cellwise, may occur together. This problem has been addressed in the multivariate scalar setting by Agostinelli et al. (2015) that propose a two steps method. In the first step, a univariate filter is used to eliminate large cellwise outliers, i.e., detection and replacement by missing values, then, in the second step, a robust estimation, specifically designed to deal with missing data, is applied to the incomplete data. Leung et al. (2016) notice that the univariate filter does not handle well moderate-size cellwise outliers, therefore they introduce for the first step a consistent bivariate filter to be used in combination with the univariate filter. Rousseeuw and Bossche (2018) propose a method for detecting deviating data cells that

takes the correlations between the variables into account, whereas, Tarr et al. (2016) devise a method for robust estimation of precision matrices under cellwise contamination. Other methods that consider cellwise outliers have been developed for regression and classification (Filzmoser et al., 2020; Aerts and Wilms, 2017).

To deal with multivariate functional outliers, in this paper we propose a new framework, referred to as robust multivariate functional control chart (RoMFCC), for SPM of multivariate functional data that is robust to both functional casewise and cellwise outliers. The latter corresponds to a contamination model where outliers arise in each variable independently from the other functional variables. Specifically, to deal with functional cellwise outliers, the proposed framework considers an extension of the filtering approach proposed by Agostinelli et al. (2015) to univariate functional data and an imputation method inspired by the robust imputation technique of Branden and Verboven (2009). Moreover, it also considers a robust multivariate functional principal component analysis (RoMFPCA) based on the ROBPCA method (Hubert et al., 2005), and a profile monitoring strategy built on the Hotelling's T^2 and the squared prediction error (SPE) control charts (Noorossana et al., 2011; Grasso et al., 2016; Centofanti et al., 2021b; Capezza et al., 2020, 2021a, 2022). A Monte Carlo simulation study is performed to quantify the probability of signal (i.e., detecting an OC observation) of RoMFCC in identifying mean shifts in the functional variables in presence of both casewise and cellwise outliers. That is, the proposed RoMFCC is compared with other control charts already present in the literature. Finally, the practical applicability of the proposed control chart is illustrated on the motivating real-case study in the automotive manufacturing industry. In particular, the RoMFCC is shown to adequately identify a drift in the manufacturing process due to electrode wear.

The article is structured as follows. Section 2 introduces the proposed RoMFCC framework. In Section 3, a simulation study is presented where RoMFCC is compared to other popular competing methods. The real-case study in the automotive industry is presented in Section 4. Section 5 concludes the article. Supplementary materials for this article are available online. All computations and plots have been obtained using the programming language R (R Core Team, 2021).

2 The Robust Multivariate Functional Control Chart Framework

The proposed RoMFCC is a new general framework for SPM of multivariate functional data that is able to deal with both functional casewise and cellwise outliers. It relies on the following four main elements.

- (I) *Functional univariate filter*, which is used to identify functional cellwise outliers to be replaced by missing components.
- (II) *Robust functional data imputation*, where a robust imputation method is applied to the incomplete data to replace missing values.
- (III) *Casewise robust dimensionality reduction*, which reduces the infinite dimensionality of the multivariate functional data by being robust towards casewise outliers.
- (IV) *Monitoring strategy*, to appropriately monitor multivariate functional data.

In what follows, we describe a specific implementation of the RoMFCC framework where (I) an extension of the filtering proposed by Agostinelli et al. (2015), referred to as functional univariate filter (FUF), is considered; (II) a robust functional data imputation method referred to as RoFDI and based on the robust imputation technique of Branden and Verboven (2009) is used; (III) the RoMFPCA is considered as the casewise robust dimensionality reduction method. Finally, (IV) the multivariate functional data are monitored through the profile monitoring approach based on the simultaneous application of the Hotelling's T^2 and the squared prediction error (SPE) control charts. For ease of presentation, the RoMFPCA is presented in Section 2.1. Then, Section 2.2, Section 2.3, and, Section 2.4 describe the FUF, the RoFDI method, and the monitoring strategy, respectively. Section 2.5 details the Phase I and Phase II of the proposed implementation of the RoMFCC framework where the elements (I-IV) are put together.

2.1 Robust Multivariate Functional Principal Component Analysis

Let $\mathbf{X} = (X_1, \dots, X_p)^T$ a random vector with realization in the Hilbert space \mathbb{H} of p -dimensional vectors of functions defined on the compact set $\mathcal{T} \in \mathbb{R}$ with realizations in $L^2(\mathcal{T})$, i.e., the Hilbert spaces of square integrable functions defined on \mathcal{T} . Accordingly, the inner product of two functions f and g in $L^2(\mathcal{T})$ is $\langle f, g \rangle = \int_{\mathcal{T}} f(t)g(t)dt$, and the norm is $\|\cdot\| = \sqrt{\langle \cdot, \cdot \rangle}$. The inner product of two function vectors $\mathbf{f} = (f_1, \dots, f_p)^T$ and $\mathbf{g} = (g_1, \dots, g_p)^T$ in \mathbb{H} is $\langle \mathbf{f}, \mathbf{g} \rangle_{\mathbb{H}} = \sum_{j=1}^p \langle f_j, g_j \rangle$ and the norm is $\|\cdot\|_{\mathbb{H}} = \sqrt{\langle \cdot, \cdot \rangle_{\mathbb{H}}}$.

We assume that \mathbf{X} has mean $\boldsymbol{\mu} = (\mu_1, \dots, \mu_p)^T$, $\mu_i(t) = \mathbb{E}(X_i(t))$, $t \in \mathcal{T}$ and covariance $\mathbf{G} = \{G_{ij}\}_{1 \leq i, j \leq p}$, $G_{ij}(s, t) = \text{Cov}(X_j(s), X_j(t))$, $s, t \in \mathcal{T}$. In what follows, to take into account for differences in degrees of variability and units of measurements among X_1, \dots, X_p , the transformation approach of Chiou et al. (2014) is considered. Specifically, let consider the vector of standardized variables $\mathbf{Z} = (Z_1, \dots, Z_p)^T$, $Z_i(t) = v_i(t)^{-1/2}(X_i(t) - \mu_i(t))$, with $v_i(t) = G_{ii}(t, t)$, $t \in \mathcal{T}$. Then, from the multivariate Karhunen-Loève's Theorem (Happ and Greven, 2018) follows that

$$\mathbf{Z}(t) = \sum_{l=1}^{\infty} \xi_l \boldsymbol{\psi}_l(t), \quad t \in \mathcal{T},$$

where $\xi_l = \langle \boldsymbol{\psi}_l, \mathbf{Z} \rangle_{\mathbb{H}}$ are random variables, said *principal components scores* or simply *scores* such that $\mathbb{E}(\xi_l) = 0$ and $\mathbb{E}(\xi_l \xi_m) = \lambda_l \delta_{lm}$, with δ_{lm} the Kronecker delta. The elements of the orthonormal set $\{\boldsymbol{\psi}_l\}$, $\boldsymbol{\psi}_l = (\psi_{l1}, \dots, \psi_{lp})^T$, with $\langle \boldsymbol{\psi}_l, \boldsymbol{\psi}_m \rangle_{\mathbb{H}} = \delta_{lm}$, are referred to as *principal components*, and are the eigenfunctions of the covariance \mathbf{C} of \mathbf{Z} corresponding to the eigenvalues $\lambda_1 \geq \lambda_2 \geq \dots \geq 0$. Following the approach of Ramsay and Silverman (2005), the eigenfunctions and eigenvalues of the covariance \mathbf{C} are estimated through a basis function expansion approach. Specifically, we assume that the functions Z_j and a generic eigenfunction $\boldsymbol{\psi}$ of \mathbf{C} with components ψ_j , for $j = 1, \dots, p$, can be represented as

$$Z_j(t) \approx \sum_{k=1}^K c_{jk} \phi_{jk}(t), \quad \psi_j(t) \approx \sum_{k=1}^K b_{jk} \phi_{jk}(t), \quad t \in \mathcal{T} \quad (1)$$

where $\boldsymbol{\phi}_j = (\phi_{j1}, \dots, \phi_{jK})^T$, $\mathbf{c}_j = (c_{j1}, \dots, c_{jK})^T$ and $\mathbf{b}_j = (b_{j1}, \dots, b_{jK})^T$ are the basis

functions and coefficient vectors for the expansion of Z_j and ψ_j , respectively. With these assumptions, standard multivariate functional principal component analysis (Ramsay and Silverman, 2005; Chiou et al., 2014) estimates eigenfunctions and eigenvalues of the covariance \mathbf{C} by performing standard multivariate principal component analysis on the random vector $\mathbf{W}^{1/2}\mathbf{c}$, where $\mathbf{c} = (\mathbf{c}_1^T, \dots, \mathbf{c}_p^T)^T$ and \mathbf{W} is a block-diagonal matrix with diagonal blocks \mathbf{W}_j , $j = 1, \dots, p$, whose entries are $w_{k_1 k_2} = \langle \phi_{k_1}, \phi_{k_2} \rangle$, $k_1, k_2 = 1, \dots, K$. Then, the eigenvalues of \mathbf{C} are estimated by those of the covariance matrix of $\mathbf{W}^{1/2}\mathbf{c}$, whereas, the components ψ_j of the generic eigenfunction, with corresponding eigenvalue λ , are estimated through Equation (1) with $\mathbf{b}_j = \mathbf{W}^{-1/2}\mathbf{u}_j$, where $\mathbf{u} = (\mathbf{u}_1^T, \dots, \mathbf{u}_p^T)^T$ is the eigenvector of the covariance matrix of $\mathbf{W}^{1/2}\mathbf{c}$ corresponding to λ . However, it is well known that standard multivariate principal component analysis is not robust to outliers (Maronna et al., 2019), which obviously reflects on the functional principal component analysis by probably providing misleading results. Extending the approach of Sawant et al. (2012) for multivariate functional data, the proposed RoMFPCA applies a robust principal component analysis alternative to the random vector $\mathbf{W}^{1/2}\mathbf{c}$. Specifically, we consider the ROBPCA approach (Hubert et al., 2005), which is a computationally efficient method explicitly conceived to produce estimates with high breakdown in high dimensional data settings, which almost always arise in the functional context, and to handle large percentage of contamination. Thus, given n independent realizations \mathbf{X}_i of \mathbf{X} , dimensionality reduction is achieved by approximating \mathbf{X}_i through $\hat{\mathbf{X}}_i$, for $i = 1, \dots, n$, as

$$\hat{\mathbf{X}}_i(t) = \hat{\boldsymbol{\mu}}(t) + \hat{\mathbf{D}}(t) \sum_{l=1}^L \hat{\xi}_{il} \hat{\boldsymbol{\psi}}_l(t) \quad t \in \mathcal{T} \quad (2)$$

where $\hat{\mathbf{D}}$ is a diagonal matrix whose diagonal entries are robust estimates $\hat{v}_j^{1/2}$ of $v_j^{1/2}$, $\hat{\boldsymbol{\mu}} = (\hat{\mu}_1, \dots, \hat{\mu}_p)^T$ is a robust estimate of $\boldsymbol{\mu}$, $\hat{\boldsymbol{\psi}}_l$ are the first L robustly estimated principal components and $\hat{\xi}_{il} = \langle \hat{\boldsymbol{\psi}}_l, \hat{\mathbf{Z}}_i \rangle_{\mathbb{H}}$ are the estimated scores with robustly estimated variances $\hat{\lambda}_l$. The estimates $\hat{\boldsymbol{\psi}}_l$ and $\hat{\lambda}_l$ are obtained through the n realizations of \mathbf{Z}_i estimated by using $\hat{\mu}_j$ and \hat{v}_j . The robust estimates $\hat{\mu}_j$ and \hat{v}_j are obtained through the scale equivariant functional M -estimator and the functional normalized median absolute deviation estimator proposed by Centofanti et al. (2021a). As in the multivariate setting, L is generally chosen

such that the retained principal components $\hat{\psi}_1, \dots, \hat{\psi}_L$ explain at least a given percentage of the total variability, which is usually in the range 70-90%, however, more sophisticated methods could be used as well, see Jolliffe (2011) for further details.

2.2 Functional Univariate Filter

To extend the filter of Agostinelli et al. (2015) and Leung et al. (2016) to univariate functional data, let consider n independent realizations X_i of a random function X with values in $L^2(\mathcal{T})$. The proposed FUF considers the functional distances D_i^{fil} , $i = 1, \dots, n$, defined as

$$D_i^{fil} = \sum_{l=1}^{L^{fil}} \frac{(\hat{\xi}_{il}^{fil})^2}{\hat{\lambda}_l^{fil}}, \quad (3)$$

where the estimated scores $\hat{\xi}_{il}^{fil} = \langle \hat{\psi}_l^{fil}, \hat{Z}_i \rangle$, the estimated eigenvalues $\hat{\lambda}_l^{fil}$, the estimated principal components $\hat{\psi}_j^{fil}$, and the estimated standardized observations \hat{Z}_i of X_i are obtained by applying, with $p = 1$, the RoMFPCA described in Section 2.1 to the sample X_i , $i = 1, \dots, n$. In this setting, RoMFPCA is used to appropriately represent distances among X_i 's and not to perform dimensionality reduction, this means that L^{fil} should be sufficiently large to capture a large percentage of the total variability δ^{fil} . Let G_n the empirical distribution of D_i^{fil} , that is

$$G_n(x) = \frac{1}{n} \sum_{i=1}^n I(D_i^{fil} \leq x), \quad x \geq 0,$$

where I is the indicator function. Then, functional observations X_i are labeled as cellwise outliers by comparing $G_n(x)$ with $G(x)$, $x \geq 0$, where G is a reference distribution for D_i^{fil} . Following Leung et al. (2016), we consider the chi-squared distribution with L^{fil} degrees of freedom, i.e., $G = \chi_{L^{fil}}^2$. The proportion of flagged cellwise outliers is defined by

$$d_n = \sup_{x \geq \eta} \{G(x) - G_n(x)\}^+,$$

where $\{a\}^+$ represents the positive part of a , and $\eta = G^{-1}(\alpha)$ is a large quantile of G . Following Agostinelli et al. (2015), in the following we consider $\alpha = 0.95$ as the aim is to detect extreme cellwise outliers, but other choices could be considered as well. Finally,

we flag $[nd_n]$ observations with the largest functional distances D_i^{fil} as functional cellwise outliers (here $[a]$ is the largest integer less than or equal to a). From the arguments in Agostinelli et al. (2015) and Leung et al. (2016) the FUF is a consistent even when the actual distribution of D_i^{fil} is unknown, that is asymptotically the filter will not wrongly flag a cellwise outlier provided that the tail of the chosen reference distribution G is heavier (or equal) than that of the actual unknown distribution.

2.3 Robust Functional Data Imputation

Let consider n independent realizations $\mathbf{X}_i = (X_{i1}, \dots, X_{ip})^T$ of a random vector of functions \mathbf{X} as defined in Section 2.1. This section considers the setting where \mathbf{X}_i , $i = 1, \dots, n$, may presents missing components, i.e., at least one of X_{i1}, \dots, X_{ip} is missing. Thus, for each realization \mathbf{X}_i we can identify the missing $\mathbf{X}_i^m = (X_{im_{i1}}, \dots, X_{im_{i_{s_i}}})^T$ and observed $\mathbf{X}_i^o = (X_{io_{i1}}, \dots, X_{io_{i_{t_i}}})^T$ components with $t_i = p - s_i$, and where $\{m_{ij}\}$ and $\{o_{ij}\}$ are disjoint set of indices, whose union coincides with the set of indices $\{1, \dots, p\}$, that indicate which components of the realization i are either observed or missing. Moreover, we assume that a set S_c of c realizations free of missing components is available. The proposed RoFDI method extends to the functional setting the robust imputation approach of Branden and Verboven (2009) that sequentially estimates the missing part of an incomplete observation such that the imputed observation has minimum distance from the space generated by the complete realizations. Analogously, starting from S_c , we propose that the missing components of the observation $\mathbf{X}_{\underline{i}} \notin S_c$, which correspond to the smallest s_i , are sequentially imputed by minimizing, with respect to $\mathbf{X}_{\underline{i}}^m$,

$$D(\mathbf{X}_{\underline{i}}^m) = \sum_{l=1}^{L^{imp}} \frac{(\hat{\xi}_{il}^{imp})^2}{\hat{\lambda}_l^{imp}}, \quad (4)$$

where the estimated scores $\hat{\xi}_{il}^{imp} = \langle \hat{\psi}_l^{imp}, \hat{\mathbf{Z}}_{\underline{i}} \rangle_{\mathbb{H}}$, eigenvalues $\hat{\lambda}_l^{imp}$, principal components $\hat{\psi}_l^{imp}$ and standardized observations $\hat{\mathbf{Z}}_{\underline{i}}$ of $\mathbf{X}_{\underline{i}}$ are obtained by applying the RoMFPCA (Section 2.1) to the free of missing data observations in S_c . Analogously to Section 2.2, RoMFPCA is used to define the distance of $\mathbf{X}_{\underline{i}}$ from the space generated by the free of missing data observations, thus, L^{imp} should be sufficiently large to capture a large

percentage of the total variability δ^{imp} . Because $\hat{\mathbf{Z}}_{\underline{i}}$ is the standardized version of $\mathbf{X}_{\underline{i}}$, we can identify the missing $\hat{\mathbf{Z}}_{\underline{i}}^m$ and observed $\hat{\mathbf{Z}}_{\underline{i}}^o$ components of $\hat{\mathbf{Z}}_{\underline{i}}$. Thus, the minimization problem in Equation (4) can be equivalently solved with respect to $\hat{\mathbf{Z}}_{\underline{i}}^m$, and the resulting solution can be unstandardized to obtain the imputed components of $\mathbf{X}_{\underline{i}}^m$.

Due to the approximations in Equation (1), $\hat{\mathbf{Z}}_{\underline{i}}$ is uniquely identified by the coefficient vectors \mathbf{c}_{ij} , $j = 1, \dots, p$, related to the basis expansions of its components. Let \mathbf{c}_{ij}^m , $j = m_{i1}, \dots, m_{is_i}$ and \mathbf{c}_{ij}^o , $j = o_{i1}, \dots, o_{it_i}$ be the coefficient vectors corresponding to the missing and observed components of $\hat{\mathbf{Z}}_{\underline{i}}$, respectively, and, $\mathbf{c}_{\underline{i}}^m = \left(\mathbf{c}_{im_{i1}}^{mT}, \dots, \mathbf{c}_{im_{is_i}}^{mT} \right)^T$ and $\mathbf{c}_{\underline{i}}^o = \left(\mathbf{c}_{io_{i1}}^{oT}, \dots, \mathbf{c}_{io_{it_i}}^{oT} \right)^T$. Moreover, let indicate with $\hat{\mathbf{b}}_{lj}$, $l = 1, \dots, L^{imp}$, $j = 1, \dots, p$, the coefficient vectors related to the basis expansions of the components of the estimated principal components $\hat{\boldsymbol{\psi}}_l^{imp}$, and with $\hat{\mathbf{B}} = \left(\hat{\mathbf{b}}_1, \dots, \hat{\mathbf{b}}_{L^{imp}} \right)$ the matrix whose columns are $\hat{\mathbf{b}}_l = \left(\hat{\mathbf{b}}_{l1}^T, \dots, \hat{\mathbf{b}}_{lp}^T \right)^T$. Then, the solution of the minimization problem in Equation (4) is

$$\hat{\mathbf{c}}_{\underline{i}}^m = -\mathbf{C}_{mm}^+ \mathbf{C}_{mo} \mathbf{c}_{\underline{i}}^o \quad (5)$$

where \mathbf{A}^+ is the Moore-Penrose inverse of the matrix \mathbf{A} , \mathbf{C}_{mm} and \mathbf{C}_{mo} are the matrices constructed by taking the columns m_{i1}, \dots, m_{is_i} and o_{i1}, \dots, o_{it_i} of the matrix composed by the rows m_{i1}, \dots, m_{is_i} of

$$\mathbf{C} = \mathbf{W} \hat{\mathbf{B}} \hat{\boldsymbol{\Lambda}}^{-1} \hat{\mathbf{B}}^T \mathbf{W}$$

with \mathbf{W} the block-diagonal matrix defined in Section 2.1, and $\hat{\boldsymbol{\Lambda}}$ the diagonal matrix whose diagonal entries are the estimated eigenvalues $\hat{\lambda}_l^{imp}$, $l = 1, \dots, L^{imp}$. Moreover, to address the correlation bias issue typical of deterministic imputation approaches (Little and Rubin, 2019; Van Buuren, 2018), we propose to impute $\mathbf{c}_{\underline{i}}^m$ through $\mathbf{c}_{\underline{i}}^{m,imp} = \left(\mathbf{c}_{i1}^{m,impT}, \dots, \mathbf{c}_{is_i}^{m,impT} \right)^T$ as follows

$$\mathbf{c}_{\underline{i}}^{m,imp} = \hat{\mathbf{c}}_{\underline{i}}^m + \boldsymbol{\varepsilon}_i \quad (6)$$

where $\boldsymbol{\varepsilon}_i$ is a multivariate normal random variable with mean zero and a residual covariance matrix robustly estimated from the regression residuals of the coefficient vectors of the missing component on those of the observed component for the observations in S_c through

the model in Equation (5). Thus, the proposed RoFDI approach is a stochastic imputation method (Little and Rubin, 2019; Van Buuren, 2018). Then, the components of $\hat{\mathbf{Z}}_{\underline{i}}^m$ are imputed, for $j = 1, \dots, s_{\underline{i}}$, as

$$\hat{Z}_{ij}^{m,imp}(t) = (\mathbf{c}_{ij}^{m,imp})^T \phi_j(t), \quad t \in \mathcal{T},$$

where ϕ_j is the vector of basis function corresponding to the j -th component of $\hat{\mathbf{Z}}$ (Section 2.1), and the imputed missing components of $\mathbf{X}_{\underline{i}}$ are obtained by unstandardizing $\hat{\mathbf{Z}}_{\underline{i}}^m$. Once the missing components of $\mathbf{X}_{\underline{i}}$ are imputed, the whole observation is added to S_c and the next observation, which does not belong to S_c and corresponds to the smallest $s_{\underline{i}}$, is considered. Similarly to Branden and Verboven (2009), if the cardinality of S_c at the first iteration is sufficiently large, we suggest to not update the RoMFPCA model each time a new imputed observation is added to S_c to avoid infeasible time complexity of the RoFDI, otherwise, the RoMFPCA model could be updated each time a given number of observations are added to S_c . Finally, to take into account the increased noise due to single imputation, the proposed RoFDI can be easily included in a multiple imputation framework (Van Buuren, 2018; Little and Rubin, 2019), indeed, differently imputed datasets may be obtained by performing several times the RoFDI due to the presence of the stochastic component ε_i in Equation (6).

2.4 The Monitoring Strategy

The (IV) element of the proposed RoMFCC implementation relies on the consolidated monitoring strategy for a multivariate functional quality characteristic \mathbf{X} based on the Hotelling's T^2 and SPE control charts. The former assesses the stability of \mathbf{X} in the finite dimensional space spanned by the first principal components identified through the RoMFPCA (Section 2.1), whereas, the latter monitors changes along directions in the complement space. Specifically, the Hotelling's T^2 statistic for \mathbf{X} is defined as

$$T^2 = \sum_{l=1}^{L^{mon}} \frac{(\xi_l^{mon})^2}{\lambda_l^{mon}},$$

where λ_l^{mon} are the variances of the scores $\xi_l^{mon} = \langle \boldsymbol{\psi}_l^{mon}, \mathbf{Z} \rangle_{\mathbb{H}}$ where \mathbf{Z} is the vector of standardized variable of \mathbf{X} and $\boldsymbol{\psi}_l^{mon}$ are the corresponding principal components as defined in Section 2.1. The number L^{mon} is chosen such that the retained principal components explain at least a given percentage δ^{mon} of the total variability. The statistic T^2 is the standardized squared distance from the centre of the orthogonal projection of \mathbf{Z} onto the principal component space spanned by $\boldsymbol{\psi}_1^{mon}, \dots, \boldsymbol{\psi}_{L^{mon}}^{mon}$. Whereas, the distance between \mathbf{Z} and its orthogonal projection onto the principal component space is measured through the SPE statistic, defined as

$$SPE = \|\mathbf{Z} - \hat{\mathbf{Z}}\|_{\mathbb{H}}^2,$$

where $\hat{\mathbf{Z}} = \sum_{l=1}^{L^{mon}} \xi_l^{mon} \boldsymbol{\psi}_l^{mon}$.

Under the assumption of multivariate normality of ξ_l^{mon} , which is approximately true by the central limit theorem (Nomikos and MacGregor, 1995), the control limits of the Hotelling's T^2 control chart can be obtained by considering the $(1 - \alpha^*)$ quantiles of a chi-squared distribution with L^{mon} degrees of freedom (Johnson et al., 2014). Whereas, the control limits for SPE control chart can be computed by using the following equation (Jackson and Mudholkar, 1979)

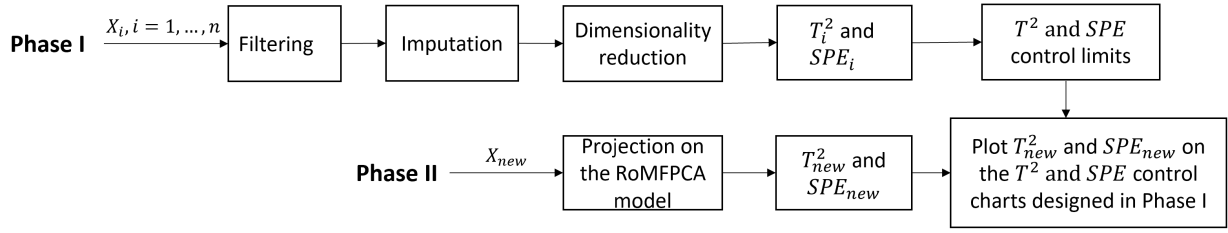
$$CL_{SPE, \alpha^*} = \theta_1 \left[\frac{c_{\alpha^*} \sqrt{2\theta_2 h_0^2}}{\theta_1} + 1 + \frac{\theta_2 h_0 (h_0 - 1)}{\theta_1^2} \right]^{1/h_0}$$

where c_{α^*} is the normal deviate corresponding to the upper $(1 - \alpha^*)$ quantile, $h_0 = 1 - 2\theta_1\theta_3/3\theta_2^2$, $\theta_j = \sum_{l=L^{mon}+1}^{\infty} (\lambda_l^{mon})^j$, $j = 1, 2, 3$. Note that, to control the family wise error rate (FWER), α^* should be chosen appropriately. We propose to use the Šidák correction $\alpha^* = 1 - (1 - \alpha)^{1/2}$ (Šidák, 1967), where α is the overall type I error probability.

2.5 The Proposed Method

The proposed RoMFCC implementation collects all the elements introduced in the previous sections for the Phase II monitoring strategy where a set of Phase I observations, which can be contaminated with both functional casewise and cellwise outliers, is used for the design of the control chart. Both phases are outlined in the scheme of Figure 2 and detailed in the following sections.

Figure 2: Scheme of the RoMFCC approach.



2.5.1 Phase I

Let \mathbf{X}_i , $i = 1, \dots, n$, the Phase I random sample of the multivariate functional quality characteristic \mathbf{X} , used to characterize the normal operating conditions of the process. It can be contaminated with both functional casewise and cellwise outliers.

In the *filtering* step, functional cellwise outliers are identified through the FUF described in Section 2.2, and, then, replaced by missing components. Note that, if cellwise outliers are identified for each component of a given observation, then, that observation is removed from the sample because its imputation does not provide any additional information for the analysis. In the *imputation* step, missing components are imputed through the RoFDI method presented in Section 2.3. Once the imputed Phase I sample is obtained, it used to estimate the RoMFPCA model and perform the *dimensionality reduction* step as described in Section 2.1. The Hotelling's T^2 and SPE statistics are, then, computed for each observation in the Phase I sample after the imputation step. Specifically, the values T_i^2 and SPE_i of the statistics are computed as described in Section 2.4 by considering the estimated RoMFPCA model obtained in the dimensionality reduction step. Finally, control limits for the Hotelling's T^2 and SPE control charts are obtained as described in Section 2.4. Note that the parameters θ_j to estimate CL_{SPE, α^*} are approximated by considering a finite summation to the maximum number of estimable principal components, which is finite for a sample of n observations. If a multiple imputation strategy is employed by performing the imputation step several times, then the multiple estimated RoMFPCA models could be combined by averaging the robustly estimated covariance functions as suggested in Van Ginkel et al. (2007).

Note that, when the sample size n is small compared to the number of process variables, undesirable effect upon the performance of the RoMFCC could arise (Ramaker et al.,

2004; Kruger and Xie, 2012). To reduce possible overfitting issues and, thus, increase the monitoring performance of the RoMFCC, a reference sample of Phase I observations, referred to as *tuning set*, could be considered, which is different from the one used in the previous steps, referred to as *training set*. Specifically, on the line of Kruger and Xie (2012), Chapter 6.4, the tuning set is passed through the filtering and imputation steps and, then, it is projected on the RoMFPCA model, estimated through the training set observations, to robustly estimate the distribution of the resulting scores. Finally, Hotelling's T^2 and SPE statistics and control charts limits are calculated by taking into account the estimated distribution of the tuning set scores.

2.5.2 Phase II

In the actual monitoring phase (Phase II), a new observation \mathbf{X}_{new} is projected on the RoMFPCA model to compute the values of T_{new}^2 and SPE_{new} statistics accordingly to the score distribution identified in Phase I. An alarm signal is issued if at least one between T_{new}^2 and SPE_{new} violates the control limits.

3 Simulation Study

The overall performance of the proposed RoMFCC is evaluated by means of an extensive Monte Carlo simulation study. The aim of this simulation is to assess the performance of the RoMFCC in identifying mean shifts of the multivariate functional quality characteristic when the Phase I sample is contaminated with both functional cellwise and casewise outliers. The data generation process (detailed in Supplementary Material A) is inspired by the real-case study in Section 4 and mimics typical behaviours of DRCs in a RSW process. Specifically, it considers a multivariate functional quality characteristic with $p = 10$ components. Two main scenarios are considered that are characterized by different Phase I sample contamination. Specifically, the Phase I sample is contaminated by functional cellwise outliers in Scenario 1 and by functional casewise outliers in Scenario 2, with a contamination probability equal to 0.05 in both cases. In the Supplementary Material B, additional results obtained by considering contamination probability equal to 0.1 are

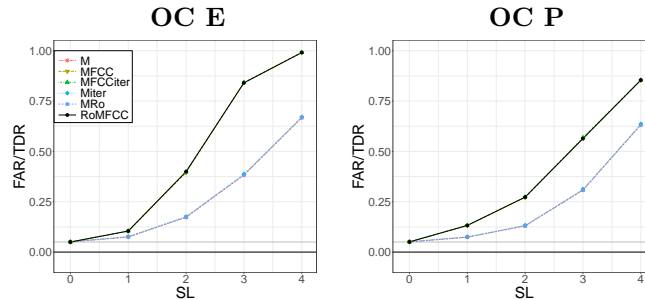
shown. For each scenario, two contamination models, referred to as Out E and Out P, with three increasing contamination levels, referred to as C1, C2 and C3, are considered. The former mimics a splash weld (expulsion), caused by excessive welding current, while the latter resembles phase shift of the peak time caused by an increased electrode force (Xia et al., 2019). Moreover, we consider also a scenario, referred to as Scenario 0, representing settings where the Phase I sample is not contaminated. To generate the Phase II sample, two types of OC conditions, referred to as OC E and OC P, are considered that are generated analogously to the two contamination models Out E and Out P, respectively, at 4 different severity levels $SL = \{1, 2, 3, 4\}$.

The proposed RoMFCC implementation is compared with several natural competing approaches. The first approaches are control charts for multivariate scalar data, built on the average value of each component of the multivariate functional data. Among them, we consider the *multivariate classical* Hotelling's T^2 control chart, referred to as M, the *multivariate iterative* variant, referred to as Miter, where outliers detected by the control chart in Phase I are iteratively removed until all data are assumed to be IC, and the *multivariate robust* control chart proposed by Chenouri et al. (2009), referred to as MRo. We further consider also two approaches recently appeared in the profile monitoring literature, i.e., the multivariate *functional control charts*, referred to as MFCC, proposed by Capezza et al. (2020, 2022), and the multivariate *iterative functional control charts* variant, referred to as MFCCiter, where outliers detected by the control chart in Phase I are iteratively removed until all data are assumed to be IC. The RoMFCC is implemented as described in Section 2 with $\delta_{fil} = \delta_{imp} = 0.999$ and $\delta_{mon} = 0.7$, and to take into account the increased noise due to single imputation, 5 differently imputed datasets are generated through RoFDI. While data are observed through noisy discrete values, each component of the generated quality characteristic observations is obtained by considering the approximation in Equation (1) with $K = 10$ cubic B-splines estimated through the spline smoothing approach based on a roughness penalty on the second derivative (Ramsay and Silverman, 2005). For each scenario, contamination model, contamination level, OC condition and severity level, 50 simulation runs are performed. Each run considers a Phase I sample of 4000 observations, where for MFCC, MFCCiter and RoMFCC, 1000 are used as training set, and the

remaining 3000 are used as tuning set. The Phase II sample is composed of 4000 i.i.d. observations. The RoMFCC and the competing methods performances are assessed by means of true detection rate (TDR), which is the proportion of points outside the control limits whilst the process is OC, and the false alarm rate (FAR), which is the proportion of points outside the control limits whilst the process is IC. The FAR should be as similar as possible to the overall type I error probability α considered to obtain the control limits and set equal to 0.05, whereas the TDR should be as close to one as possible.

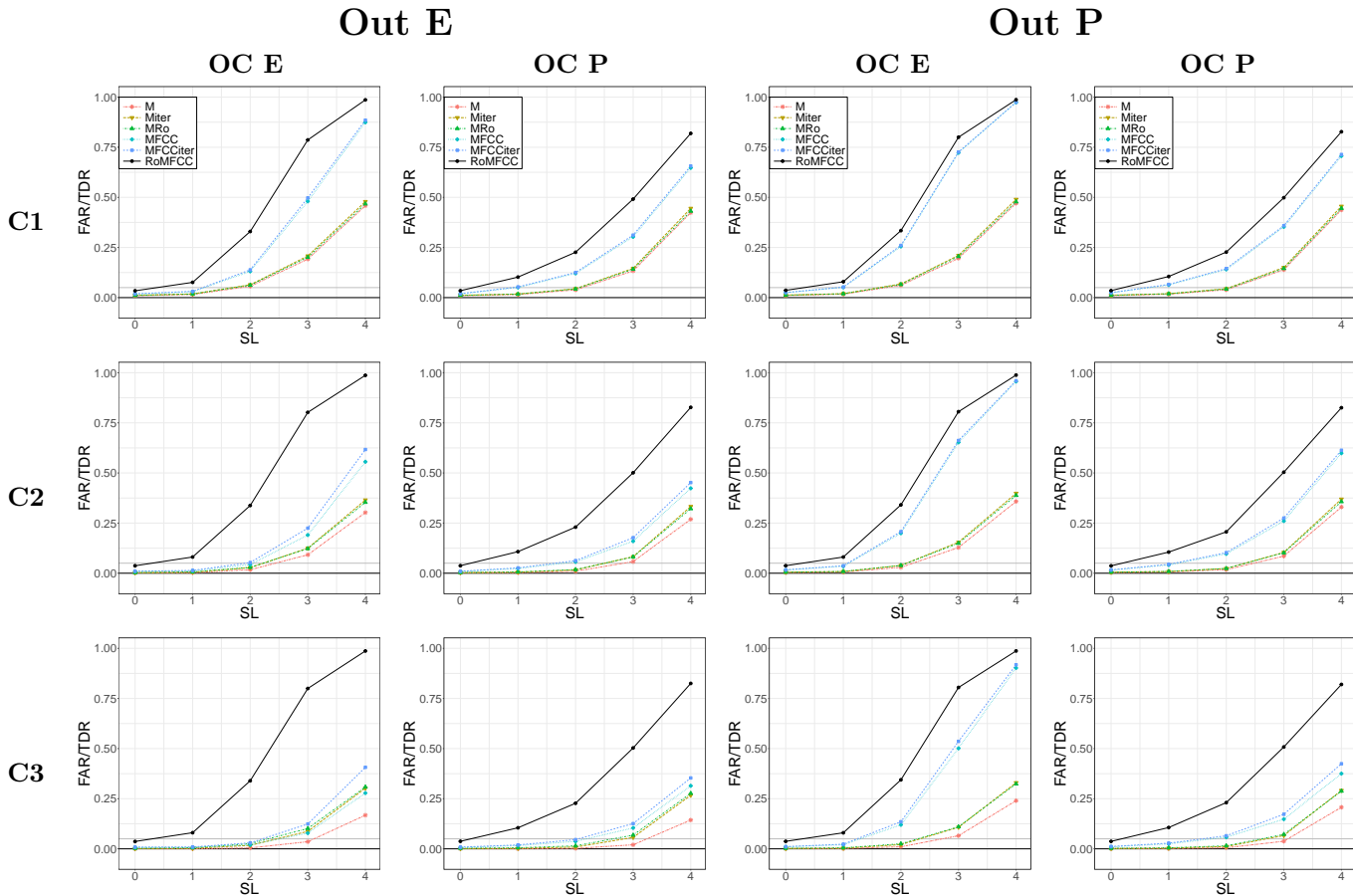
Figure 3-5 display for Scenario 0, Scenario 1 and Scenario 2, respectively, as a function of the severity level SL , the mean FAR ($SL = 0$) or TDR ($SL \neq 0$) for each OC condition OC E and OC P, contamination level C1, C2 and C3 and contamination model Out E and Out P.

Figure 3: Mean FAR ($SL = 0$) or TDR ($SL \neq 0$) achieved by M, Miter, MRo, MFCC, MFCCiter and RoMFCC for each OC condition (OC E and OC P) as a function of the severity level SL in Scenario 0.



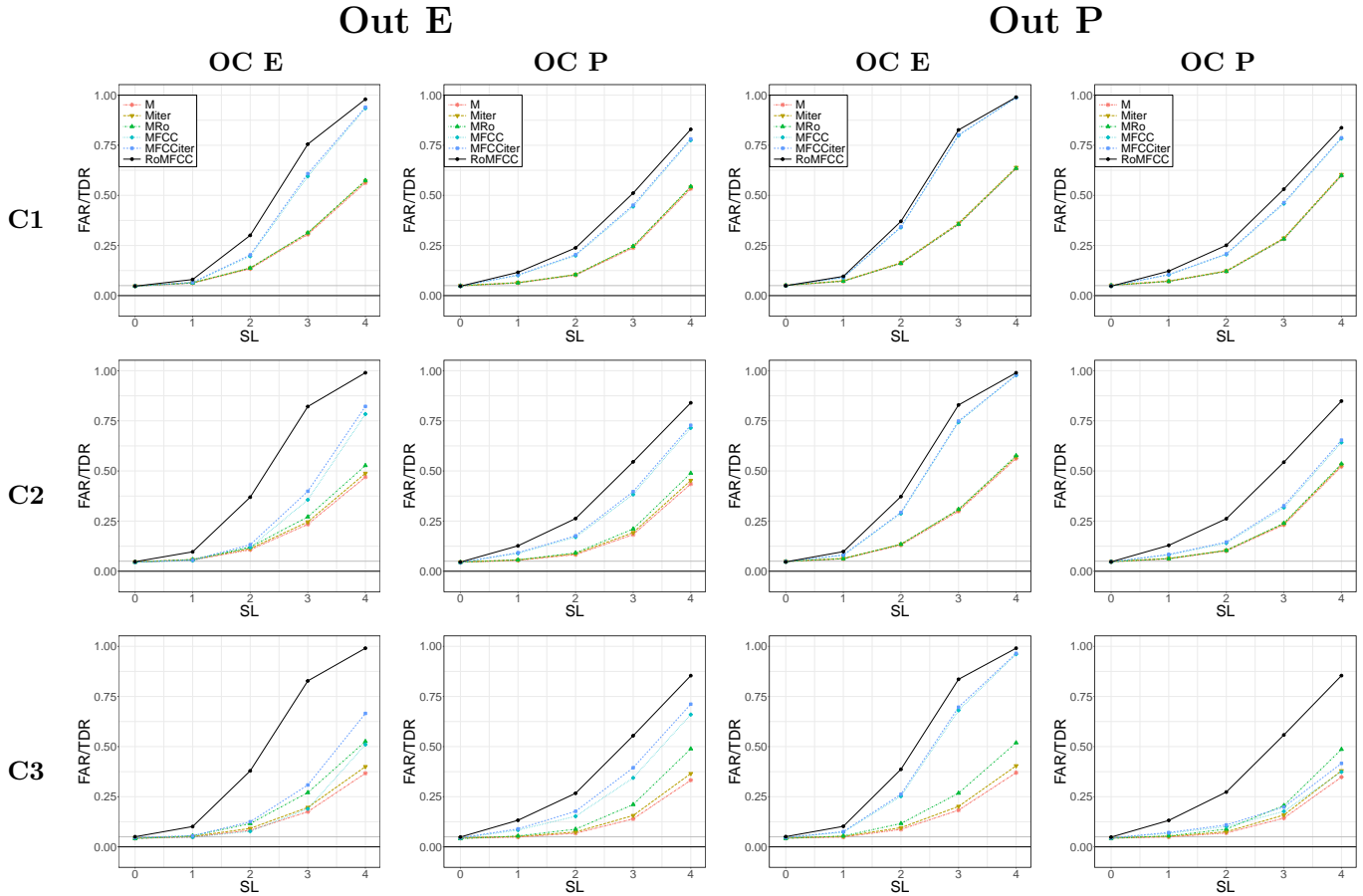
When the Phase I sample is not contaminated by outliers, Figure 3 shows that all the approaches that take into account the functional nature of the data, i.e., MFCC, MFCCiter, RoMFCC, achieve the same performance for both OC conditions. Although this setting should be not favourable to approaches specifically designed to deal with outliers, MFCCiter and RoMFCC perform equal to MFCC. The non-functional approaches, i.e., M, Miter, MRo, show worse performance than the functional counterparts, and there is no significant performance difference among them as well. Figure 4 show the results for Scenario 1, where the Phase I sample is contaminated by cellwise outliers. The proposed RoMFCC largely outperforms the competing methods for each contamination model, contamination level and OC condition. As expected, as the contamination level increases the differences in performance between the RoMFCC and the competing methods increase as well. Indeed, the performance of RoMFCC is almost insensible to the contamination lev-

Figure 4: Mean FAR ($SL = 0$) or TDR ($SL \neq 0$) achieved by M, Miter, MRo, MFCC, MFCCiter and RoMFCC for each contamination level (C1, C2 and C3), OC condition (OC E and OC P) as a function of the severity level SL with contamination model Out E and Out P in Scenario 1.



els as well as the contamination models, differently from the competing methods whose performance decreases as the contamination level increases and the contamination model changes. Moreover, the MFCCiter, which is representative of the baseline method in this setting, only slightly improves the performance of the MFCC. This is probably due to the masking effect that prevents the MFCCiter to iteratively identify functional cellwise outlier in the Phase I sample and, thus, makes it equivalent to MFCC. The performance of the non-functional methods are totally unsatisfactory because they are not able to both capture the functional nature of the data and successfully deal with functional cellwise outliers. Specifically, M is the worst method overall readily followed by Miter and MRo. Furthermore, as the contamination level increases, the competing functional methods lose their favourable performance and tend to achieve performance comparable to the non-functional approaches. This shows that if outliers are not properly dealt with, terrible performance

Figure 5: Mean FAR ($SL = 0$) or TDR ($SL \neq 0$) achieved by M, Miter, MRo, MFCC, MFCCiter and RoMFCC for each contamination level (C1, C2 and C3), OC condition (OC E and OC P) as a function of the severity level SL with contamination model Out E and Out P in Scenario 2.



could arise independently of the suitability of the methods considered.

From Figure 5, also in Scenario 2, RoMFCC is clearly the best method. However, in this scenario the difference in performance between the RoMFCC and the competing methods is less pronounced than in Scenario 1. This is expected because the Phase I sample is now contaminated by functional casewise outliers, which is the only contamination type against which the competing methods are able to provide a certain degree of robustness. Note that, the performance of RoMFCC are almost unaffected by contamination in the Phase I sample also in this scenario, which proves the ability of the proposed method to deal with both functional cellwise and casewise outliers.

4 Real-Case Study

To demonstrate the potential of the proposed RoMFCC in practical situations, a real-case study in the automotive industry is presented henceforth. As introduced in Section 1, it addresses the issue of monitoring the quality of the RSW process, which guarantees the structural integrity and solidity of welded assemblies in each vehicle (Martín et al., 2014). The RSW process (Zhang and Senkara, 2011) is an autogenous welding process in which two overlapping conventional steel galvanized sheets are joint together, without the use of any filler material. Joints are formed by applying pressure to the weld area from two opposite sides by means of two copper electrodes. Voltage applied to the electrodes generates a current flowing between them through the material. The electrical current flows because the resistance offered by metals causes significant heat generation (Joule effect) that increases the metal temperature at the faying surfaces of the work pieces up to the melting point. Finally, due to the mechanical pressure of the electrodes, the molten metal of the jointed metal sheets cools and solidifies, forming the so-called weld nugget (Raoelison et al., 2012). To monitor the RSW process, the modern automotive Industry 4.0 framework allows the automatic acquisition of a large volume of process parameters. The DRC is considered the most important of these parameters to describe the quality of the RSW process. Further details on how the typical behaviour of a DRC is related to the physical and metallurgical development of a spot weld are provided by Capezza et al. (2021b).

Data analyzed in this study are courtesy of Centro Ricerche Fiat and are recorded at the Mirafiori Factory during lab tests and are acquired during RSW processes made on the body of the Fiat 500BEV. A body is characterized by a large number of spot welds with different characteristics, e.g, the thickness and material of the sheets to be joined together and the welding time. In this paper, we focus on monitoring a set of ten spot welds made on the body by one of the welding machines. Therefore, for each sub-assembly the multivariate functional quality characteristic is a vector of the ten DRCs, corresponding to the the second welding pulse of ten spot welds normalized on the time domain $[0, 1]$, for a total number of assemblies equal to 1839. Moreover, resistance measurements were collected at a regular grid of points equally spaced by 1 ms.

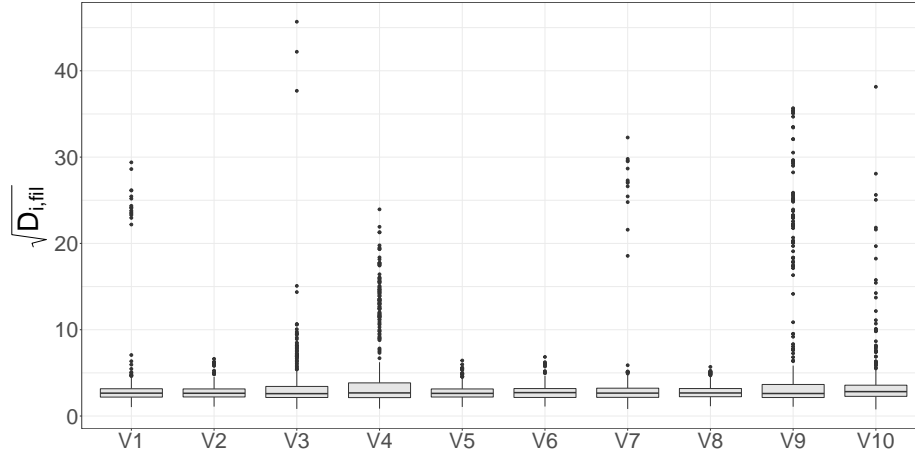


Figure 6: Boxplot of the functional distance square roots $\sqrt{D_{i,fil}}$ (Equation (3)) obtained from the FUF applied on the training set.

The RSW process quality is directly affected by electrode wear since the increase in weld numbers leads to changed electrical, thermal and mechanical contact conditions at electrode and sheet interfaces (Manladan et al., 2017). Thus, to take into account the wear issue, electrodes go through periodical renovations. In this setting, a paramount issue refers to the swift identification of DRCs mean shifts caused by electrode wear, which could be considered as a criterion for electrode life termination and guide the electrode renovation strategy.

In the light of this, the 919 multivariate profiles corresponding to spot welds made immediately before electrode renewal are used to form the Phase I sample, whereas, the remaining 920 observations are used in Phase II to evaluate the proposed chart performance. We expect that the mean shift of the Phase II DRCs caused by electrode wear should be effectively captured by the proposed control chart. The RoMFCC is implemented as in the simulation study in Section 3 with the training and tuning sets, each composed by 460 Phase I observations, randomly selected without remittance. As shown in Figure 1 of Section 1, data are plausibly contaminated by several outliers. This is further confirmed by Figure 6, which shows the boxplot of the functional distance square roots $\sqrt{D_{i,fil}}$ (Equation (3)) obtained from the FUF applied on the training set. Some components clearly show the presence of functional cellwise outliers that are possibly arranged in groups, while other components seem less severely contaminated. Figure 7 shows the application of the

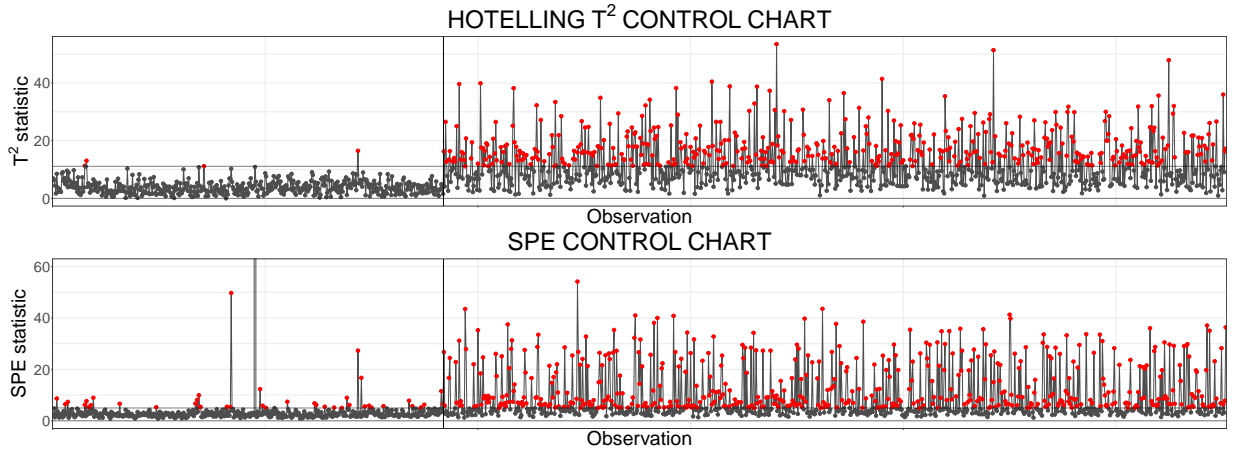


Figure 7: Hotelling’s T^2 and SPE control charts for the RoMFCC in the real-case study. The vertical line separates the monitoring statistics calculated for the tuning set, on the left, and the Phase II data set on the right, while the horizontal lines define the control limits.

proposed RoMFCC. The vertical line separates the monitoring statistics calculated for the tuning set, on the left, and the Phase II data set on the right, while the horizontal lines define the control limits. Note that, a significant number of tuning set observations are signaled as OC, highlighted in red in Figure 7. This is expected because these points may include functional casewise outlier not filtered out by the FUF. In the monitoring phase, many points are signaled as OCs by the RoMFCC. In particular, the RoMFCC signals 72.3% of the observations in the Phase II data set as OC. This shows that the proposed method is particularly sensible to mean shifts caused by an increased electrode wear.

Finally, the proposed method is compared with the competing methods presented in the simulation study in Section 3. Table 1 shows the estimated TDR values \widehat{TDR} on the Phase II sample for all the considered competing methods. Similarly to Centofanti et al. (2021b), the uncertainty of \widehat{TDR} is quantified through a bootstrap analysis (Efron and Tibshirani, 1994). Table 1 reports the mean \overline{TDR} of the empirical bootstrap distribution of \widehat{TDR} , and the corresponding bootstrap 95% confidence interval (CI) for each monitoring method. The bootstrap analysis shows that the RoMFCC outperforms the competing control charts, indeed bootstrap 95% confidence intervals are strictly above those of all considered monitoring approaches. As in Section 3, non-functional approaches, i.e., M, Miter, MRo, show worse performance than the functional counterparts because they are not able to satisfactorily capture the functional nature of the data and robust approaches always improve the non-robust ones. Therefore, the proposed RoMFCC stands out as the

	\widehat{TDR}	\overline{TDR}	CI
M	0.336	0.335	[0.305,0.368]
Miter	0.462	0.461	[0.428,0.496]
MRo	0.513	0.512	[0.481,0.547]
MFCC	0.541	0.541	[0.511,0.574]
MFCCiter	0.632	0.632	[0.595,0.664]
RoMFCC	0.723	0.723	[0.695,0.753]

Table 1: Estimated TDR values $T\hat{D}R$ on the Phase II sample, mean \overline{TDR} of the empirical bootstrap distribution of $T\hat{D}R$, and the corresponding bootstrap 95% confidence interval (CI) for each monitoring method in the real-case study.

best method to promptly identify OC conditions in the RWS process caused by an increased electrode wear with a Phase I sample contaminated by functional outliers.

5 Conclusions

In this paper, we propose a new robust framework for the statistical process monitoring of multivariate functional data, referred to as *robust multivariate functional control charts* (RoMFCC). The RoMFCC is designed to assess the presence of assignable causes of variation while being robust to both functional casewise and cellwise outliers. The proposed method is suitable for those industrial processes where many functional variables are available and occasional outliers are produced, such as anomalies in the data acquisition and data collected during a fault in the process. Specifically, the RoMFCC framework is based on four main elements, i.e. a functional univariate filter to identify functional cellwise outliers, to be replaced by missing values, a robust functional data imputation of these missing values, a casewise robust dimensionality reduction based on ROBPCA and a monitoring strategy based on the Hotelling's T^2 and SPE control charts. These elements are combined in a Phase II monitoring strategy where a set of Phase I observations, which can be contaminated with both functional casewise and cellwise outliers, is used for the design of the control chart.

To the best of the authors' knowledge, the RoMFCC framework is the first monitoring scheme that is able to monitor a multivariate functional quality characteristic while being robust to functional casewise and cellwise outliers. Indeed, methods already present in the literature either apply robust approaches to multivariate scalar features extracted from the profiles or use diagnostic approaches on the multivariate functional data to iteratively

remove outliers. However, the former are not able to capture the functional nature of the data, while the latter are not able to deal with functional cellwise outliers.

The performance of the RoMFCC framework is assessed through an extensive Monte Carlo simulation study where it is compared with several competing monitoring methods for multivariate scalar data and multivariate functional data. The ability of the proposed method to estimate the distribution of the data without removing observations while being robust to both functional casewise and cellwise outliers allows the RoMFCC to outperform the competitors in all the considered scenarios. Lastly, the practical applicability of the proposed method is illustrated through a motivating real-case study, which addresses the issue of monitoring the quality of a resistance spot-welding process in the automotive industry. Also in this case, the RoMFCC shows better performance than the competitors in the identification of out-of-control condition of the dynamic resistance curves.

Supplementary Materials

The Supplementary Materials contain additional details about the data generation process in the simulation study (A), additional simulation results (B), as well as the R code to reproduce graphics and results over competing methods in the simulation study.

Acknowledgments

The present work was developed within the activities of the project ARS01_00861 “Integrated collaborative systems for smart factory - ICOSAF” coordinated by CRF (Centro Ricerche Fiat Scpa - www.crf.it) and financially supported by MIUR (Ministero dell’Istruzione, dell’Università e della Ricerca).

References

Aerts, S. and Wilms, I. (2017). Cellwise robust regularized discriminant analysis. *Statistical Analysis and Data Mining: The ASA Data Science Journal*, 10(6):436–447.

- Agostinelli, C., Leung, A., Yohai, V. J., and Zamar, R. H. (2015). Robust estimation of multivariate location and scatter in the presence of cellwise and casewise contamination. *Test*, 24(3):441–461.
- Alemán-Gómez, Y., Arribas-Gil, A., Desco, M., Elías, A., and Romo, J. (2022). Depthgram: Visualizing outliers in high-dimensional functional data with application to fmri data exploration. *Statistics in Medicine*.
- Alfaro, J. and Ortega, J. F. (2009). A comparison of robust alternatives to hotelling’s t^2 control chart. *Journal of Applied Statistics*, 36(12):1385–1396.
- Alqallaf, F., Van Aelst, S., Yohai, V. J., and Zamar, R. H. (2009). Propagation of outliers in multivariate data. *The Annals of Statistics*, pages 311–331.
- Arribas-Gil, A. and Romo, J. (2014). Shape outlier detection and visualization for functional data: the outliergram. *Biostatistics*, 15(4):603–619.
- Boente, G. and Salibián-Barrera, M. (2021). Robust functional principal components for sparse longitudinal data. *Metron*, 79(2):159–188.
- Branden, K. V. and Verboven, S. (2009). Robust data imputation. *Computational Biology and Chemistry*, 33(1):7–13.
- Cabana, E. and Lillo, R. E. (2021). Robust multivariate control chart based on shrinkage for individual observations. *Journal of Quality Technology*, pages 1–26.
- Capezza, C., Centofanti, F., Lepore, A., Menafoglio, A., Palumbo, B., and Vantini, S. (2021a). Functional regression control chart for monitoring ship CO_2 emissions. *Quality and Reliability Engineering International*, 38(3):1519–1537.
- Capezza, C., Centofanti, F., Lepore, A., Menafoglio, A., Palumbo, B., and Vantini, S. (2022). funcharts: Control charts for multivariate functional data in r.
- Capezza, C., Centofanti, F., Lepore, A., and Palumbo, B. (2021b). Functional clustering methods for resistance spot welding process data in the automotive industry. *Applied Stochastic Models in Business and Industry*, 37(5):908–925.
- Capezza, C., Lepore, A., Menafoglio, A., Palumbo, B., and Vantini, S. (2020). Control charts for monitoring ship operating conditions and CO_2 emissions based on scalar-on-function regression. *Applied Stochastic Models in Business and Industry*, 36(3):477–500.

- Centofanti, F., Colosimo, B. M., Grasso, M. L., Menafoglio, A., Palumbo, B., and Vantini, S. (2021a). Robust functional anova with application to additive manufacturing.
- Centofanti, F., Lepore, A., Menafoglio, A., Palumbo, B., and Vantini, S. (2021b). Functional regression control chart. *Technometrics*, 63(3):281–294.
- Chenouri, S., Steiner, S. H., and Variyath, A. M. (2009). A multivariate robust control chart for individual observations. *Journal of Quality Technology*, 41(3):259–271.
- Chiou, J.-M., Chen, Y.-T., and Yang, Y.-F. (2014). Multivariate functional principal component analysis: A normalization approach. *Statistica Sinica*, pages 1571–1596.
- Cuesta-Albertos, J. A. and Fraiman, R. (2006). Impartial trimmed means for functional data. *DIMACS Series in Discrete Mathematics and Theoretical Computer Science*, 72:121.
- Cuevas, A. and Fraiman, R. (2009). On depth measures and dual statistics. a methodology for dealing with general data. *Journal of Multivariate Analysis*, 100(4):753–766.
- Dai, W. and Genton, M. G. (2018). Multivariate functional data visualization and outlier detection. *Journal of Computational and Graphical Statistics*, 27(4):923–934.
- Dickinson, D., Franklin, J., Stanya, A., et al. (1980). Characterization of spot welding behavior by dynamic electrical parameter monitoring. *Welding Journal*, 59(6):170.
- Efron, B. and Tibshirani, R. J. (1994). *An introduction to the bootstrap*. CRC press.
- Febrero, M., Galeano, P., and González-Manteiga, W. (2008). Outlier detection in functional data by depth measures, with application to identify abnormal nox levels. *Environmetrics: The official journal of the International Environmetrics Society*, 19(4):331–345.
- Filzmoser, P., Höppner, S., Ortner, I., Serneels, S., and Verdonck, T. (2020). Cellwise robust m regression. *Computational Statistics & Data Analysis*, 147:106944.
- Fraiman, R. and Muniz, G. (2001). Trimmed means for functional data. *Test*, 10(2):419–440.
- Grasso, M., Menafoglio, A., Colosimo, B. M., and Secchi, P. (2016). Using curve-registration information for profile monitoring. *Journal of Quality Technology*, 48(2):99–127.
- Happ, C. and Greven, S. (2018). Multivariate functional principal component analysis for data observed on different (dimensional) domains. *Journal of the American Statistical Association*, 113(522):649–659.

- Hubert, M., Rousseeuw, P. J., and Segaert, P. (2015). Multivariate functional outlier detection. *Statistical Methods & Applications*, 24(2):177–202.
- Hubert, M., Rousseeuw, P. J., and Vanden Branden, K. (2005). Robpca: a new approach to robust principal component analysis. *Technometrics*, 47(1):64–79.
- Hyndman, R. J. and Shang, H. L. (2010). Rainbow plots, bagplots, and boxplots for functional data. *Journal of Computational and Graphical Statistics*, 19(1):29–45.
- Hyndman, R. J. and Ullah, M. S. (2007). Robust forecasting of mortality and fertility rates: A functional data approach. *Computational Statistics & Data Analysis*, 51(10):4942–4956.
- Jackson, J. E. and Mudholkar, G. S. (1979). Control procedures for residuals associated with principal component analysis. *Technometrics*, 21(3):341–349.
- Jensen, W. A., Birch, J. B., and Woodall, W. H. (2007). High breakdown estimation methods for phase i multivariate control charts. *Quality and Reliability Engineering International*, 23(5):615–629.
- Johnson, R. A., Wichern, D. W., et al. (2014). *Applied multivariate statistical analysis*, volume 6. Pearson London, UK:.
- Jolliffe, I. (2011). *Principal component analysis*. Springer.
- Kokoszka, P. and Reimherr, M. (2017). *Introduction to functional data analysis*. Chapman and Hall/CRC.
- Kordestani, M., Hassanvand, F., Samimi, Y., and Shahriari, H. (2020). Monitoring multivariate simple linear profiles using robust estimators. *Communications in Statistics-Theory and Methods*, 49(12):2964–2989.
- Kruger, U. and Xie, L. (2012). *Statistical monitoring of complex multivariate processes: with applications in industrial process control*. John Wiley & Sons.
- Lee, S., Shin, H., and Billor, N. (2013). M-type smoothing spline estimators for principal functions. *Computational Statistics & Data Analysis*, 66:89–100.
- Leung, A., Zhang, H., and Zamar, R. (2016). Robust regression estimation and inference in the presence of cellwise and casewise contamination. *Computational Statistics & Data Analysis*, 99:1–11.

- Little, R. J. and Rubin, D. B. (2019). *Statistical analysis with missing data*, volume 793. John Wiley & Sons.
- Locantore, N., Marron, J., Simpson, D., Tripoli, N., Zhang, J., Cohen, K., Boente, G., Fraiman, R., Brumback, B., Croux, C., et al. (1999). Robust principal component analysis for functional data. *Test*, 8(1):1–73.
- López-Pintado, S. and Romo, J. (2011). A half-region depth for functional data. *Computational Statistics & Data Analysis*, 55(4):1679–1695.
- Manladan, S., Yusof, F., Ramesh, S., Fadzil, M., Luo, Z., and Ao, S. (2017). A review on resistance spot welding of aluminum alloys. *The International Journal of Advanced Manufacturing Technology*, 90(1):605–634.
- Maronna, R. A., Martin, R. D., Yohai, V. J., and Salibián-Barrera, M. (2019). *Robust statistics: theory and methods (with R)*. John Wiley & Sons.
- Martín, Ó., Pereda, M., Santos, J. I., and Galán, J. M. (2014). Assessment of resistance spot welding quality based on ultrasonic testing and tree-based techniques. *Journal of Materials Processing Technology*, 214(11):2478–2487.
- Menafoglio, A., Grasso, M., Secchi, P., and Colosimo, B. M. (2018). Profile monitoring of probability density functions via simplicial functional pca with application to image data. *Technometrics*, 60(4):497–510.
- Moheghi, H., Noorossana, R., and Ahmadi, O. (2020). Phase i and phase ii analysis of linear profile monitoring using robust estimators. *Communications in Statistics-Theory and Methods*, pages 1–18.
- Montgomery, D. C. (2012). *Introduction to Statistical Quality Control*. Wiley.
- Nomikos, P. and MacGregor, J. F. (1995). Multivariate spc charts for monitoring batch processes. *Technometrics*, 37(1):41–59.
- Noorossana, R., Saghaei, A., and Amiri, A. (2011). *Statistical analysis of profile monitoring*, volume 865. John Wiley & Sons.
- R Core Team (2021). *R: A Language and Environment for Statistical Computing*. R Foundation for Statistical Computing, Vienna, Austria.
- Ramaker, H.-J., van Sprang, E. N., Westerhuis, J. A., and Smilde, A. K. (2004). The effect of the

- size of the training set and number of principal components on the false alarm rate in statistical process monitoring. *Chemometrics and intelligent laboratory systems*, 73(2):181–187.
- Ramsay, J. O. and Silverman, B. W. (2005). *Functional Data Analysis*. Springer.
- Raoelison, R., Fuentes, A., Rogeon, P., Carre, P., Loulou, T., Carron, D., and Dechalotte, F. (2012). Contact conditions on nugget development during resistance spot welding of zn coated steel sheets using rounded tip electrodes. *Journal of Materials Processing Technology*, 212(8):1663–1669.
- Rousseeuw, P. J. (1984). Least median of squares regression. *Journal of the American statistical association*, 79(388):871–880.
- Rousseeuw, P. J. and Bossche, W. V. D. (2018). Detecting deviating data cells. *Technometrics*, 60(2):135–145.
- Sawant, P., Billor, N., and Shin, H. (2012). Functional outlier detection with robust functional principal component analysis. *Computational Statistics*, 27(1):83–102.
- Šidák, Z. (1967). Rectangular confidence regions for the means of multivariate normal distributions. *Journal of the American Statistical Association*, 62(318):626–633.
- Sinova, B., Gonzalez-Rodriguez, G., and Van Aelst, S. (2018). M-estimators of location for functional data. *Bernoulli*, 24(3):2328–2357.
- Tarr, G., Müller, S., and Weber, N. C. (2016). Robust estimation of precision matrices under cellwise contamination. *Computational Statistics & Data Analysis*, 93:404–420.
- Van Buuren, S. (2018). *Flexible imputation of missing data*. CRC press.
- Van Ginkel, J. R., Van der Ark, L. A., Sijtsma, K., and Vermunt, J. K. (2007). Two-way imputation: A bayesian method for estimating missing scores in tests and questionnaires, and an accurate approximation. *Computational Statistics & Data Analysis*, 51(8):4013–4027.
- Vargas, N. J. A. (2003). Robust estimation in multivariate control charts for individual observations. *Journal of Quality Technology*, 35(4):367–376.
- Xia, Y.-J., Su, Z.-W., Li, Y.-B., Zhou, L., and Shen, Y. (2019). Online quantitative evaluation of expulsion in resistance spot welding. *Journal of Manufacturing Processes*, 46:34–43.
- Zhang, H. and Senkara, J. (2011). *Resistance welding: fundamentals and applications*. CRC press.

Zhou, K. and Cai, L. (2014). Study on effect of electrode force on resistance spot welding process.
Journal of applied physics, 116(8):084902.

Supplementary Materials to “Robust Multivariate Functional Control Charts”

Christian Capezza¹, Fabio Centofanti ^{*1}, Antonio Lepore¹, and Biagio
Palumbo¹

¹*Department of Industrial Engineering, University of Naples Federico II, Piazzale Tecchio 80,
80125, Naples, Italy*

arXiv:2207.07978v1 [stat.AP] 16 Jul 2022

*Corresponding author. e-mail: fabio.centofanti@unina.it

Table 1. Bessel correlation function and parameter for data generation in the simulation study.

	ρ	ν
$J_\nu(z) = \left(\frac{ z }{2}\right)^\nu \sum_{j=0}^{\infty} \frac{(-(z /\rho)^2/4)^j}{j!\Gamma(\nu+j+1)}$	0.125	0

A Details on Data Generation in the Simulation Study

The data generation process is inspired by the real-case study in Section 4 and mimics typical behaviours of DRCs in a RSW process. The data correlation structure is generated similar to Centofanti et al. (2021); Chiou et al. (2014). The compact domain \mathcal{T} is set, without loss of generality, equal to $[0, 1]$ and the number components p is set equal to 10. The eigenfunction set $\{\boldsymbol{\psi}_i\}$ is generated by considering the correlation function \mathbf{G} through the following steps.

1. Set the diagonal elements G_{ll} , $l = 1, \dots, p$ of \mathbf{G} as the *Bessel* correlation function of the first kind (Abramowitz and Stegun, 1964). The general form of the correlation function and parameter used are listed in Table 1. Then, calculate the eigenvalues $\{\eta_{lk}^X\}$ and the corresponding eigenfunctions $\{\vartheta_{lk}\}$, $k = 1, 2, \dots$, of G_{ll} , $l = 1, \dots, p$.
2. Obtain the cross-correlation function G_{lj} , $l, j = 1, \dots, p$ and $l \neq j$, by

$$G_{lj}(t_1, t_2) = \sum_{k=1}^{\infty} \frac{\eta_k}{1 + |l - j|} \vartheta_{lk}(t_1) \vartheta_{jk}(t_2) \quad t_1, t_2 \in \mathcal{T}. \quad (\text{A.1})$$

3. Calculate the eigenvalues $\{\lambda_i\}$ and the corresponding eigenfunctions $\{\boldsymbol{\psi}_i\}$ through the spectral decomposition of $\mathbf{G} = \{G_{lj}\}_{l,j=1,\dots,p}$, for $i = 1, \dots, L^*$.

Further, L^* is set equal to 10. Let $\mathbf{Z} = (Z_1, \dots, Z_p)$ as

$$\mathbf{Z} = \sum_{i=1}^{L^*} \xi_i \boldsymbol{\psi}_i. \quad (\text{A.2})$$

with $\boldsymbol{\xi}_{L^*} = (\xi_1^X, \dots, \xi_{L^*}^X)^T$ generated by means of a multivariate normal distribution with covariance $\text{Cov}(\boldsymbol{\xi}_{L^*}^X) = \mathbf{\Lambda}^{\mathbf{X}} = \text{diag}(\lambda_1, \dots, \lambda_{L^*})$.

Furthermore, let the mean process m

$$m(t) = 0.2074 + 0.3117 \exp(-371.4t) + 0.5284(1 - \exp(0.8217t)) - 423.3 [1 + \tanh(-26.15(t + 0.1715))] \quad t \in \mathcal{T}. \quad (\text{A.3})$$

Note that, the mean function m is generated to resemble a typical DRC through the phenomenological model for the RSW process presented in Schwab et al. (2012). Then, the contamination models C_E and C_P , which mimics a splash weld (expulsion) and phase shift of the peak time, are respectively defined as

$$C_E(t) = \min \left\{ 0, -2M_E(t - 0.5) \right\} \quad t \in \mathcal{T}, \quad (\text{A.4})$$

and

$$C_P(t) = -m(t) - (M_P/20)t + 0.2074 + 0.3117 \exp(-371.4h(t)) + 0.5284(1 - \exp(0.8217h(t))) - 423.3 [1 + \tanh(-26.15(h(t) + 0.1715))] \quad t \in \mathcal{T}, \quad (\text{A.5})$$

where $h : \mathcal{T} \rightarrow \mathcal{T}$ transforms the temporal dimension t as follows

$$h(t) = \begin{cases} t & \text{if } t \leq 0.05 \\ \frac{0.55 - M_P}{0.55}t - \left(1 + \frac{0.55 - M_P}{0.55}\right)0.05 & \text{if } 0.05 < t \leq 0.6 \\ \frac{0.4 + M_P}{0.4}t + 1 - \frac{0.4 + M_P}{0.4} & \text{if } t > 0.6, \end{cases} \quad (\text{A.6})$$

and M_E and M_P are contamination sizes. Then, $\mathbf{X} = (X_1, \dots, X_p)^T$ is obtained as follows

$$\mathbf{X}(t) = \mathbf{m}(t) + \mathbf{Z}(t)\sigma + \boldsymbol{\varepsilon}(t) + B_E \mathbf{C}_E(t) + B_P \mathbf{C}_P(t) \quad t \in \mathcal{T}, \quad (\text{A.7})$$

where \mathbf{m} is a p dimensional vector with components equal to m , $\sigma > 0$, $\boldsymbol{\varepsilon} = (\varepsilon_1, \dots, \varepsilon_p)^T$, where ε_i are white noise functions such that for each $t \in [0, 1]$, $\varepsilon_i(t)$ are normal random variables with zero mean and standard deviation σ_e , and B_{CaE} and B_{CaP} are two indepen-

Table 2. Parameters used to generate the Phase I sample in Scenario 1 and Scenario 2 of the simulation study.

	Scenario 1				Scenario 1			
	Out E		Out P		Out E		Out P	
	M_E	M_P	M_E	M_P	M_E	M_P	M_E	M_P
	$p_{CaE} = p_{CaP} = 1,$ $p_{CeE} = \tilde{p}, p_{CeP} = 0$		$p_{CaE} = p_{CaP} = 1,$ $p_{CeE} = 0, p_{CeP} = \tilde{p}$		$p_{CaE} = \tilde{p}, p_{CaP} = 0,$ $p_{CeE} = p_{CeP} = 1$		$p_{CaE} = 0, p_{CaP} = \tilde{p},$ $p_{CeE} = p_{CeP} = 1$	
C1	0.04	0.00	0.00	0.40	0.02	0.00	0.00	0.20
C2	0.06	0.00	0.00	0.45	0.03	0.00	0.00	0.30
C3	0.08	0.00	0.00	0.50	0.04	0.00	0.00	0.40

Table 3. Parameters used to generate the Phase II sample for OC E and OC P and severity level $SL = \{0, 1, 2, 3, 4\}$ in the simulation study.

SL	OC E		OC P	
	M_E	M_P	M_E	M_P
	0	0.00	0.00	0.00
1	0.01	0.00	0.00	0.20
2	0.02	0.00	0.00	0.27
3	0.03	0.00	0.00	0.34
4	0.04	0.00	0.00	0.40

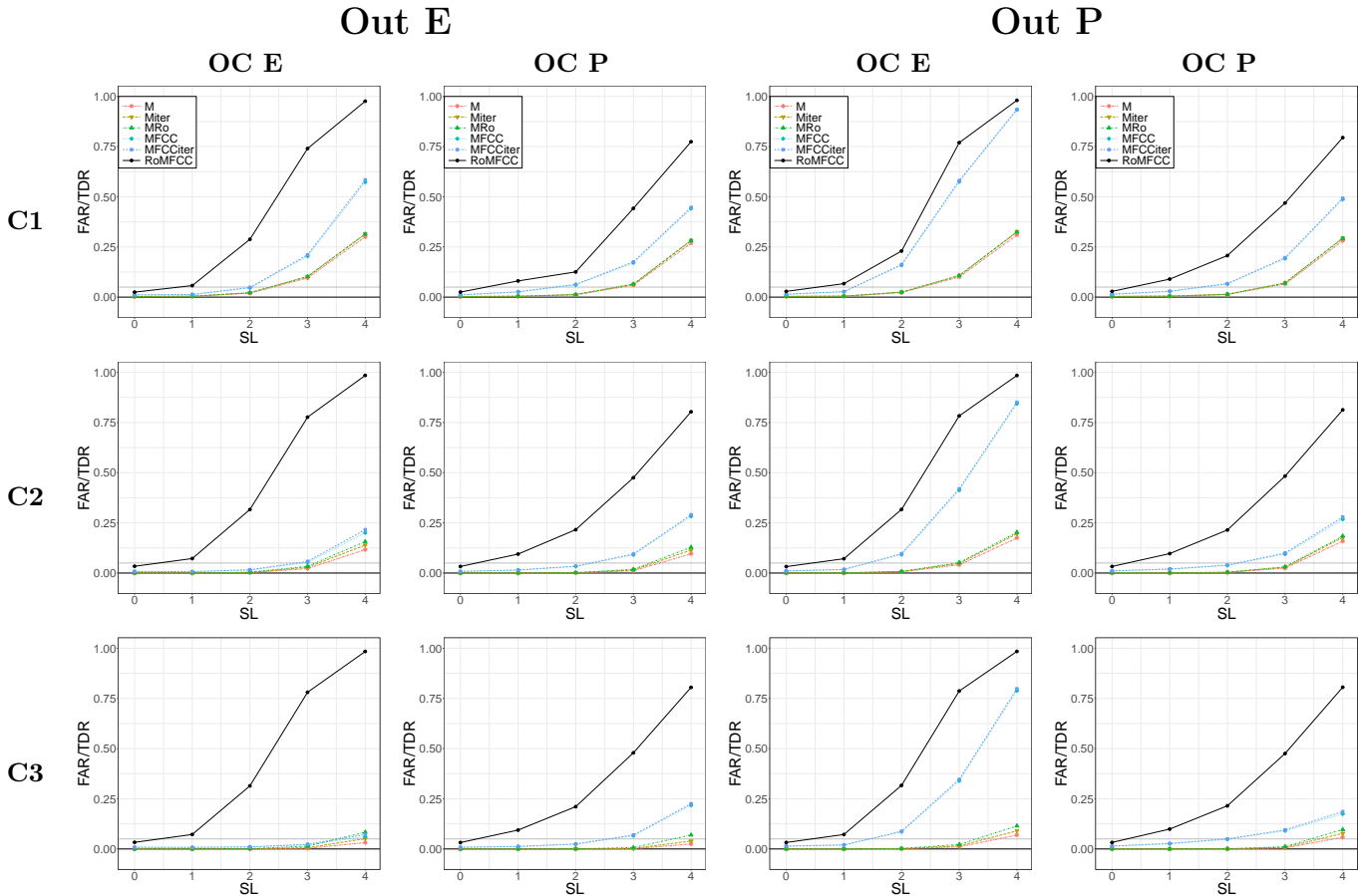
dent random variables following Bernoulli distributions with parameters p_{CaE} and p_{CaP} , respectively. Moreover, $\mathbf{C}_E = (B_{1,CeE}C_E, \dots, B_{p,CeE}C_E)^T$ and $\mathbf{C}_P = (B_{1,CeP}C_P, \dots, B_{p,CeP}C_P)^T$, where $\{B_{i,CeE}\}$ and $\{B_{i,CeP}\}$ are two sets of independent random variables following Bernoulli distributions with parameters p_{CeE} and p_{CeP} , respectively.

Then, the Phase I and Phase II samples are generated through Equation (A.7) by considering the parameters listed in Table 2 and Table 3, respectively, with $\sigma_e = 0.0025$ and $\sigma = 0.01$. The parameter \tilde{p} is the probability of contamination that for the data analysed in Section 3 and Supplementary Material B is set equal to 0.05 and 0.1, respectively. Moreover, in Scenario 0 of the simulation study data are generated through $p_{CaE} = p_{CaP} = p_{CeE} = p_{CeP} = 0$. Finally, the generate data are assumed to be discretely observed at 100 equally spaced time points over the domain $[0, 1]$.

B Additional Simulation Results

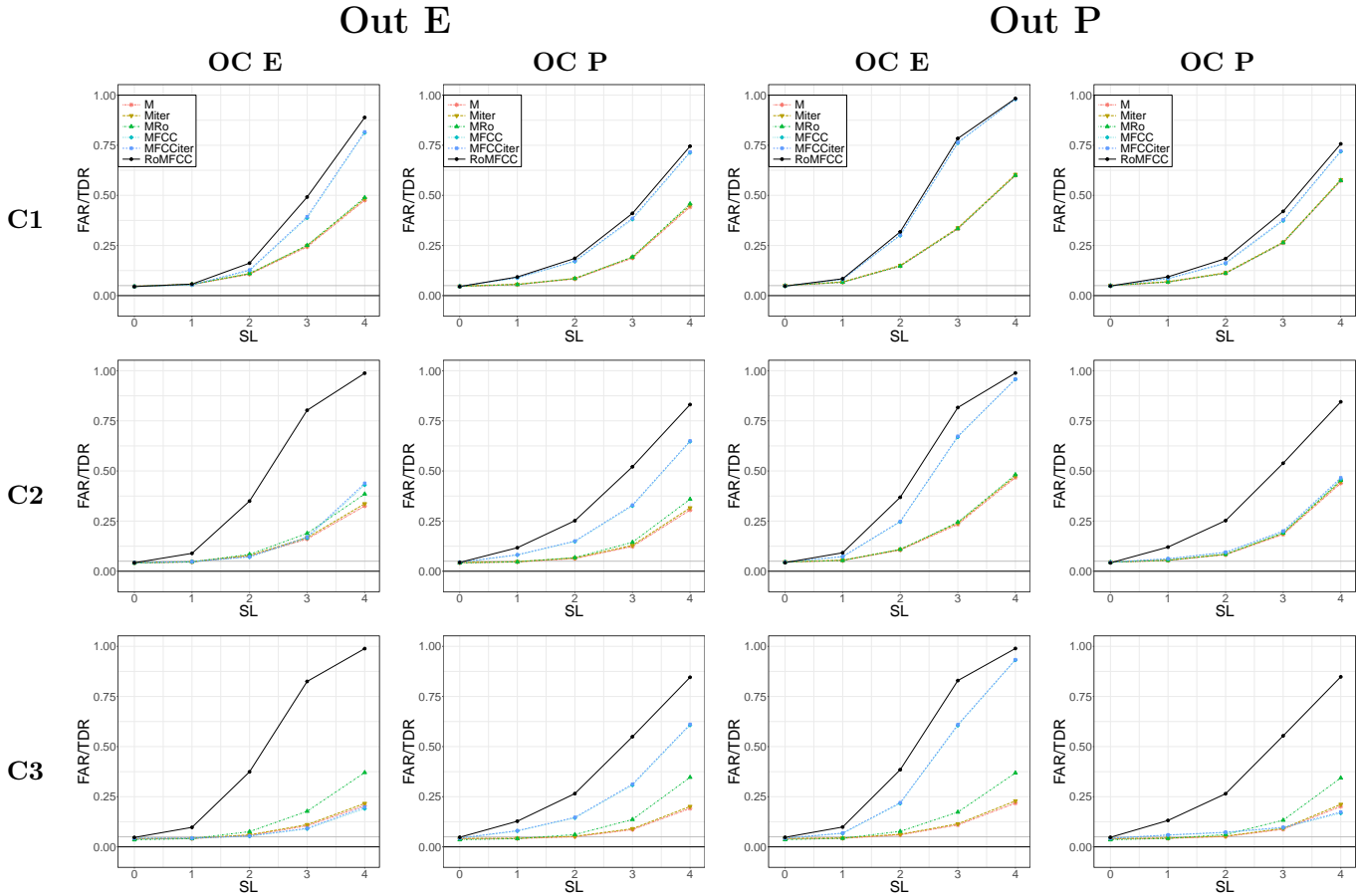
In this section, we present additional simulations to analyse the performance of the RoMFCC and the competing methods methods when data are generated as described in Supplementary Material A with probability of contamination \tilde{p} equals to 0.1. The RoMFCC is implemented as described in Section 3. Figure A.1 and Figure A.2 show for Scenario 1 and Scenario 2 the mean FAR ($SL = 0$) or TDR ($SL \neq 0$) achieved by M, Miter, MRo, MFCC, MFCCiter and RoMFCC for each contamination level (C1, C2 and C3), OC condition (OC E and OC P) as a function of the severity level SL with contamination model Out E and Out P.

Figure A.1. Mean FAR ($SL = 0$) or TDR ($SL \neq 0$) achieved by M, Miter, MRo, MFCC, MFCCiter and RoMFCC for each contamination level (C1, C2 and C3), OC condition (OC E and OC P) as a function of the severity level SL with contamination model Out E and Out P in Scenario 1 for $\tilde{p} = 0.1$.



By comparing Figure A.1 and Figure A.2 with Figure 4 and Figure 5, the RoMFCC confirms itself as the best method in all the considered settings. Specifically, the proposed method, differently from the competing methods, is almost insensible to the fact that a

Figure A.2. Mean FAR ($SL = 0$) or TDR ($SL \neq 0$) achieved by M, Miter, MRo, MFCC, MFCCiter and RoMFCC for each contamination level (C1, C2 and C3), OC condition (OC E and OC P) as a function of the severity level SL with contamination model Out E and Out P in Scenario 2 for $\tilde{p} = 0.1$.



large fraction of the data in the Phase I sample is now composed by either cellwise or case wise outliers. On the contrary, the competing methods are strongly affected by the different probability of contamination and show overall worse performance than in Section 3 and, thus, are totally inappropriate to monitor the multivariate functional quality characteristic in this setting. This further confirms as shown in Section 3, i.e., in this simulation study the RoMFCC performance is almost independent of the contamination of the Phase I sample.

As in Section 3, also in this case, performance differences between the proposed and competing methods are less pronounced in Scenario 2 due to the less severe contamination produced by functional casewise outliers. However, RoMFCC still outperforms all the competing methods and, thus, stand out as the best method.

References

- Abramowitz, M. and I. A. Stegun (1964). Handbook of mathematical functions: with formulas, graphs, and mathematical tables.
- Centofanti, F., A. Lepore, A. Menafoglio, B. Palumbo, and S. Vantini (2021). Functional regression control chart. *Technometrics* 63(3), 281–294.
- Chiou, J.-M., Y.-T. Chen, and Y.-F. Yang (2014). Multivariate functional principal component analysis: A normalization approach. *Statistica Sinica*, 1571–1596.
- Schwab, I., M. Senn, and N. Link (2012). Improving expert knowledge in dynamic process monitoring by symbolic regression. In *2012 Sixth International Conference on Genetic and Evolutionary Computing*, pp. 132–135. IEEE.